Quasiparticle relaxation dynamics in underdoped $Bi_2Sr_2CaCu_2O_{8+\delta}$ by two-color pump-probe spectroscopy

Y. Toda,[1,2] T. Mertelj,[1] P. Kusar,[1] T. Kurosawa,[3] M. Oda,[3] M. Ido,[3] and D. Mihailovic[1]
[1]*Complex Matter Department, Jozef Stefan Institute, Jamova 39, Ljubljana, SI-1000, Slovenia*
[2]*Department of Applied Physics, Hokkaido University, Sapporo 060-8628, Japan*
[3]*Department of Physics, Hokkaido University, Sapporo 060-0810, Japan*
(Received 21 April 2011; revised manuscript received 23 October 2011; published 21 November 2011)

We investigate the relaxation dynamics of photoexcited quasiparticles (QPs) in underdoped $Bi_2Sr_2CaCu_2O_{8+\delta}$ ($T_c = 78$ K). By changing the excitation energy and polarization of the probe beam, two different types of relaxation dynamics, associated with superconducting (SC) and pseudogap (PG) QPs, are quantitatively analyzed independently. From the temperature dependencies, we obtained the SC gap, $\Delta_{SC}(0) = 24$ meV, using BCS-type temperature-dependent gap and the pseudogap, $\Delta_{PG} = 41$ meV. The pump fluence ($\mathcal{F}$) dependence of the SC-dominated transients shows a contribution of the PG component above the saturation condition of the SC component ($\mathcal{F}_{th} = 16\ \mu J/cm^2$), where Cooper pairs with long-range order are fully destroyed within the photoexcited volume. Assuming a temperature-independent PG decay time, we successfully isolate the native SC transient even above $\mathcal{F}_{th}$ by subtracting the PG response from the original data. In the saturation regime, the exponential decay (recovery of SC) is fast ($\tau_{SC} \sim 2$–3 ps), suggesting an efficient nonequilibrium phonon relaxation in this compound. We also find a flat-top response preceding the exponential decay at $\mathcal{F} > \mathcal{F}_{th}$, which appears as a delay of SC recovery in the original data. This response is visible over the whole temperature range below T_c and its duration increases with increasing $\mathcal{F}$. The response is attributable to a photoinduced SC to non-SC phase transition arising from excitation by the nonthermal QPs and/or high-frequency phonons. The consistently near-constant magnitude of the PG response at the start of the SC state recovery from the non-SC phase suggests a correlation between the SC and PG QPs.

DOI: 10.1103/PhysRevB.84.174516 PACS number(s): 74.25.Gz, 78.47.jg, 74.72.Kf

I. INTRODUCTION

The coexistence of superconducting (SC) gap and pseudogap (PG) is a fascinating feature in high-T_c superconductors, and underdoped $Bi_2Sr_2CaCu_2O_{8+\delta}$ (UD-Bi2212) is one of the most extensively studied cuprates from this point of view.[1] Scanning tunneling microscopy/spectroscopy (STM/STS) and angle-resolved photoemission spectroscopy (ARPES) are the two major techniques of investigating the connection between SC and PG, where the former characterizes the spatial variations of the gaps, while the latter characterizes their momentum distributions. The recent STS and ARPES studies on UD-Bi2212 and Bi2201 (La) reveal that the SC gap located in the nodal region starts to open below T_c, while the PG shows no clear change across T_c.[2–4]

Time-resolved optical spectroscopy provides another way to resolve the quasiparticles (QPs) associated with SC and PG in the time domain.[5] Although momentum integrated energy spectra around the Fermi energy are often broad and featureless in superconductors, QP dynamics with femtosecond resolution allows us to separate the overlapping contributions more easily. Furthermore, nonequilibrium condition achieved by ultrashort pulse laser has a potential to directly reveal the pairing dynamics in time. The photoinduced vaporization of the SC condensate has been realized recently.[6] For Bi2212, an ultrafast depletion of the SC condensate on a picosecond (ps) time scale has been demonstrated.[7]

In this kind of experiments, the optical pump-probe method is typically employed, where the nonequilibrium dynamics of QPs induced by an intense pump pulse is traced by a probe pulse with a variable delay time between the two pulses. The pump pulse with an energy higher than the energy gap of SC/PG can be utilized to break Cooper pairs into QPs excited into nonequilibrium high-energy states. The nonequilibrium carriers immediately relax down to states near the gap via electron-electron and electron-phonon scattering, resulting in quasiequilibrium populations of QPs and high-frequency phonons. They then reach equilibrium by high-frequency phonon decay. A theoretical framework for analyzing the transient data has being established on the basis of comprehensive and systematic experiments on various superconductors[5,8–11] involving BCS-type,[12] cuprates,[6,7,13–26] Fe-based superconductors,[27] and other related compounds.[28] In the cuprates, the distinction of the QP dynamics between SC and PG has been realized by the characteristics of each dynamics, such as relaxation time, temperature dependence,[12–14,16–19] or dependence on the external fields.[20] The differences in transition probability and matrix elements for optical probe transitions also provide a possibility to selectively enhance the QP dynamics detection of SC/PG, which allows us to analyze each dynamics individually.[17,22]

In our previous paper, we selectively isolated the transient dynamics associated with SC and PG QPs in UD-Bi2212 by changing the probe beam energy and polarization.[22] We also showed that two distinct components can be detected simultaneously below T_c. However, the paper lacked quantitative details. In this paper, we report experimental studies on UD-Bi2212 by using a similar selective method as before. The photoexcitation with a low-repetition-rate laser allows quantitative analysis of the dynamics with high precision. In addition to the temperature dependence, we carry out the pump fluence dependence of the dynamics. At fluences where the

SC component is saturated, the PG component rises above the SC signal. At the same time, a delay of SC recovery appears and increases linearly with increasing pump fluence. We also extract the saturated SC dynamics by subtracting the PG component obtained above T_c from the original data. The response is clearly visible even in the vicinity of T_c, indicating a SC to non-SC phase transition with an efficient nonthermal phonon distribution.

II. EXPERIMENTAL

The sample used in this work was underdoped Bi2212 single crystal with $T_c \approx 78$ K grown by the traveling solvent floating zone method. The time-resolved reflectivity change ΔR was measured using a two-color pump-probe setup and was carried out with a freshly cleaved sample mounted in an optical liquid-He flow cryostat. The two pulses were derived from a 250-kHz Ti:sapphire regenerative amplifier (RegA) and a signal of an optical parametric amplifier (OPA) pumped by RegA. Due to the low repetition rate, we can neglect the laser heating, as justified in Sec. III A from the data obtained at various fluences. We employed a combination of the excitation energies (wavelengths) of 1.55 eV (800 nm) and 0.95 eV (1300 nm), where the latter energy is slightly lower than that used in the previous report (~1.07 eV).[22] Depending on the measurement, either 1.55/0.95 eV or vice versa were used for the pump/probe energy (E_{pu}/E_{pr}). The pump and probe beams were coaxially overlapped and focused onto the ab plane of the crystal by a lens ($f = 50$ mm) located on-axis, allowing for the precise spatial overlap between the beams. The beam diameters from RegA and OPA were measured to be 30 and 40 μm at the sample position, respectively. In most cases, the collinearly polarized pump and probe beams were set to be parallel to a axis of the crystal ($\mathbf{E_{pu}} \parallel \mathbf{E_{pr}} \parallel a$). The fluence of the pump beam ($\mathcal{F}$) ranged from 9 to ~900 μJ/cm^2. We set the probe fluence about three orders of magnitude smaller than the pump. Owing to the energy difference between the pump and probe beams, we can spectroscopically distinguish the reflection beams for detection. The time resolution was estimated to be around 75 fs from cross correlation measurements.

III. RESULTS AND DISCUSSIONS

A. Temperature dependence

In Fig. 1, we plot the temperature dependence of $\Delta R/R$ transients at various excitation conditions at low excitation fluences. The upper panels show the density plots of the data, where the red and blue correspond to positive and negative signs of ΔR, respectively. With excitation/probe energies of $E_{pu}/E_{pr} = 0.95/1.55$ eV [see Figs. 1(a) and 1(d)], only a negative $\Delta R/R$ transient is present below T_c, characteristic of the QP relaxation associated with the SC state. No remarkable polarization dependence was observed with this pump-probe energy combination. In contrast, a positive component is dominant in the reverse combination; $E_{pu}/E_{pr} = 1.55/0.95$ eV [see Figs. 1(b) and 1(c)]. This component remains constant across T_c, then decreases monotonically with further increasing temperature, and finally disappears around $T^* \approx 180 \sim 210$ K. Thus we assign the positive $\Delta R/R$ transient to QP relaxation associated with the PG. In the case of $\mathbf{E_{pr}} \parallel a$ probe polarization [see Figs. 1(c) and 1(f)], an additional small negative component appears in the temperature region below T_c, which can be identified as a small contribution of the SC component observed in Figs. 1(a) and 1(d). On the other hand, the negative component is nearly absent and only the positive component is apparent when $\mathbf{E_{pr}} \parallel b$ [see Figs. 1(b) and 1(e)].

As shown in Figs. 1(d) and 1(e), $\Delta R/R$ transients are well reproduced by a single exponential relaxation (thin solid lines), ensuring that we can uniquely evaluate the relaxation dynamics

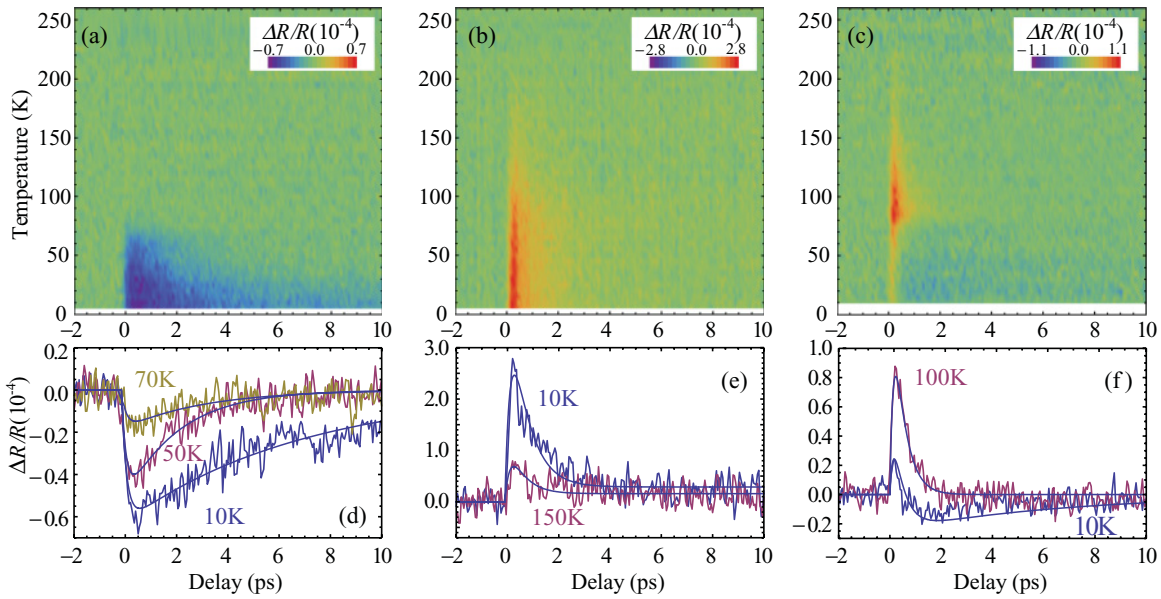

FIG. 1. (Color online) (Top) Density plots of $\Delta R/R$ transients as a function of temperature, obtained at (a) $E_{pr}/E_{pu} = 1.55/0.95$ eV (800/1300 nm) with $\mathcal{F} = 9$ μJ/cm^2 and (b) and (c) $E_{pr}/E_{pu} = 0.95/1.55$ eV (1300/800 nm). $\mathcal{F} = 75$ μJ/cm^2 and $\mathbf{E_{pr}} \parallel a$ in (b) and $\mathcal{F} = 25$ μJ/cm^2 and $\mathbf{E_{pr}} \parallel b$ in (c). (Bottom) Corresponding $\Delta R/R$ transients at typical temperatures.

of the SC and PG QPs at each excitation condition. Let us briefly comment on the selectivity of SC/PG component in the optical pump-probe measurement. In cuprates superconductors, a two-component signal consisting of SC and PG components has been widely observed,[12–14,16–19] where the magnitude of the signal reflects the change of the interband transition probabilities induced by the photoexcited QPs.[17] Since the transition probability depends on the probe energy and polarization, we can enhance/suppress one of the SC/PG components by changing the excitation condition.[22] Since $\Delta R/R$ in each component shows a similar magnitude $\sim 10^{-4}$ at the lowest temperature, which is comparable to the typical value obtained in other cuprates,[7,14,17] it is possible to consider that the photoinduced change of the transition probabilities for PG (SC) component is strongly reduced in (d) [(e)], resulting in a single exponential relaxation with SC (PG). We emphasize that there should exist a small contribution from the minority [PG in (d) and SC in (e)] in each excitation condition, but its magnitude is negligibly small as compared with the dominant signal. This is consistent with the fact that we see a small contribution of SC component below T_c in Figs. 1(c) and 1(f), where the change of probe polarization breaks the balance to cancel out the SC component owing to the dipole matrix element for the transition. The two-component signal is also seen in the SC-dominated transients when increasing the pump fluence above the saturation of SC component, which will be discussed later and in Sec. III B in more detail.

To quantitatively confirm the assignment of SC and PG components, we plot in Fig. 2 the T dependencies of $\Delta R/R$ amplitudes together with the fits (thin solid lines) characterized by the SC gap Δ_{SC} and pseudogap Δ_{PG}. Assuming sufficiently weak photoexcitation (so that the photoinduced QPs and phonon occupations are small compared to their equilibrium concentrations) and a momentum-independent gap, $\Delta R/R$ amplitude is given by[5]

$$\frac{\Delta R}{R} \propto \left[\Delta_{SC}(T) + \frac{k_B T}{2}\right]^{-1} \times \left\{1 + g\sqrt{\frac{k_B T}{\Delta_{SC}(T)}}\exp\left[-\frac{\Delta_{SC}(T)}{k_B T}\right]\right\}^{-1}, \quad (1)$$

where g represents the ratio of bosonic and electronic density of states that contribute the photoinduced QP density. We used BCS-type $\Delta_{SC}(T)$ and obtained $\Delta_{SC}(0) = 24$ meV, which is slightly larger than the values obtained from other experiments, but still consistent by taking into account the variation in the momentum space.[1,4] The agreement with the data is also good enough to ensure the identification of the SC component. For the PG component, assuming the strong bottleneck condition (QP relaxation is governed by the hot phonon relaxation) and weak photoexcitation, $\Delta R/R$ amplitude is given by[8,9]

$$\frac{\Delta R}{R} \propto \left[1 + \frac{2\nu k_B T}{N(0)\hbar\Omega_c}\exp\left(-\frac{\Delta_{PG}}{k_B T}\right)\right]^{-1}, \quad (2)$$

where $N(0) \approx 2\ \mathrm{eV}^{-1}\mathrm{cell}^{-1}\mathrm{spin}^{-1}$ is the electronic density of states per unit cell[29] and ν and Ω_c are, respectively, the number of bosons in the PG relaxation and their cutoff frequency. The best fit to the data at $\mathbf{E_{pr}} \parallel a$ (open circles) with Eq. (2) using T-independent Δ_{PG} shows $\Delta_{PG} = 41$ meV, which is also consistent with the value obtained from the STS.[4] In the same figure, we plot the amplitude of $\Delta R/R$ at $\mathbf{E_{pr}} \parallel b$ (triangles) whose T dependence is consistent with the data at $\mathbf{E_{pr}} \parallel a$ and its fitting curve.

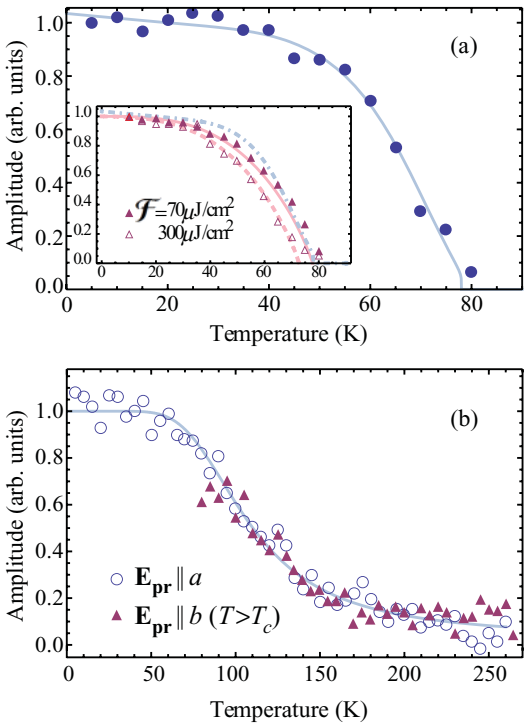

FIG. 2. (Color online) Temperature dependencies of normalized amplitudes of $\Delta R/R$ obtained from (a) $E_{pu}/E_{pr} = 0.95/1.55$ eV [data extracted from Fig. 1(a)] and from (b) $E_{pu}/E_{pr} = 1.55/0.95$ eV, [from Figs. 1(b) and 1(c)]. The thin lines in (a) and (b) are the fits by Eqs. (1) and (2), using BCS-type $\Delta_{SC}(T)$ and T-independent Δ_{PG}, respectively. Inset shows two data sets at higher fluences, where the fitting curve of (a) is reproduced as a dot-dashed line. The solid and dashed lines are given by Eq. (3), where the dashed line is obtained by shifting the solid line by -5 K.

In order to check the amount of sample heating from the laser, we compare the T dependencies of SC amplitudes measured at various pump fluences [inset of Fig. 2(a)]. Here, the fluences of the two data sets correspond to $\mathcal{F}$ above saturation condition for SC component (where the SC condensate is temporally destructed, see Sec. III B). A similar T_c was found at $\mathcal{F} = 70\ \mu\mathrm{J/cm}^2$ (closed triangles) while a small ($\sim$5 K) apparent shift of T_c due to the laser heating is observed at $\mathcal{F} = 300\ \mu\mathrm{J/cm}^2$ (open triangles). This implies that the laser heating is negligibly small for $\mathcal{F}$ up to a few hundred $\mu\mathrm{J/cm}^2$.

Under the saturation condition, the assumption of weak photoexcitation in Eq. (1) is no longer valid. Instead, we employ the Mattis-Bardeen (MB) formula to characterize the data, which are given by[6,30]

$$\frac{\Delta R}{R} \propto \Delta_{SC}(T)^2 \ln\left[\frac{\hbar\omega}{\Delta_{SC}(T)}\right], \quad (3)$$

where $\hbar\omega$ is the photon energy. This formula represents a T-dependent difference in reflectivity between the normal (non-SC) and SC states and an assumption that the reflectivity in

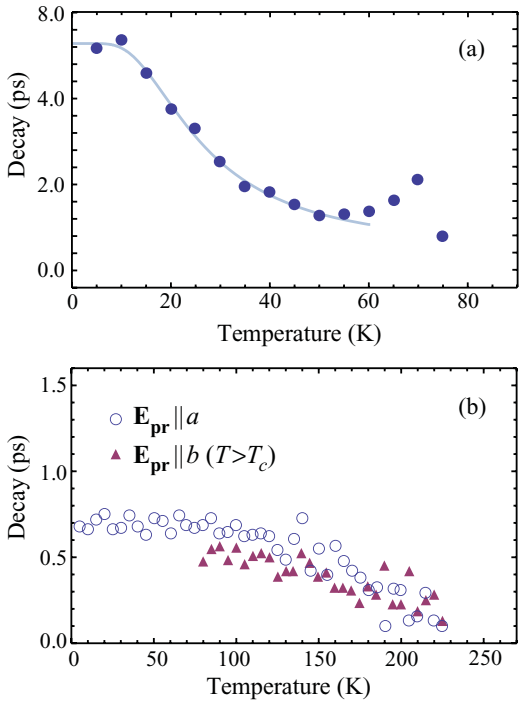

FIG. 3. (Color online) Temperature dependencies of decay time obtained from (a) $E_{pu}/E_{pr} = 0.95/1.55$ eV [from Fig. 1(a)] and (b) $E_{pu}/E_{pr} = 1.55/0.95$ eV [circles and triangles are from Figs. 1(b) and 1(c), respectively].

the non-SC state does not depend (or weakly depends) on temperature. We see a good agreement with the data at $\mathcal{F} = 70\ \mu\text{J/cm}^2$. Note that the comparison with the fit by Eq. (1) (dot-dashed line) shows a noticeable difference between low-$\mathcal{F}$ and high-$\mathcal{F}$ amplitudes. On the other hand, the data obtained far above the saturation ($\mathcal{F} = 300\ \mu\text{J/cm}^2$, open triangles) are slightly shifted downward at each temperature, suggesting that the heating by the laser may occur. Indeed, the MB fit by shifting the temperature by ~5 K shows excellent agreement with the data (dashed line in the inset).

For completion of the analysis, we plot the decay times of SC and PG components at the low fluence as a function of temperature in Figs. 3(a) and 3(b), respectively. Analogous to the amplitude, the decay time in each component shows a significantly different T dependence. The SC decay time (τ_{SC}) shows a remarkable T dependence: with increasing temperature below T_c, τ_{SC} first decreases, then reaches a minimum value of ~2 ps, and then shows a divergent-like increase as the temperature approaches T_c. Although the decay times are different, qualitatively similar T dependencies have been observed in various types of superconductors,[8,12,14,18,19,25,27] clearly indicating the universal nature of superconductors. In contrast to the characteristic T dependence of τ_{SC}, the decay time of the PG component (τ_{PG}) shows a featureless dependence (τ_{PG} gradually varies around 0.7 ps below ~100 K) in Fig. 3(b). This featureless T dependence is also consistent with τ_{PG} observed in other cuprates.[7,13–22] The decay time of $\Delta R/R$ at $\mathbf{E_{pr}} \| b$ (triangles), where we expect the single PG component above T_c, is also plotted in Fig. 3(b). The consistency of the decay time [as well as the amplitude in Fig. 2(b)] at different polarizations manifests the assignment of PG.

We now characterize τ_{SC} on the basis of Rothwarf-Taylor (RT) model in the strong bottleneck regime. At the temperature below T_c, QP relaxation rate (τ_{SC}^{-1}) is given by[8,18]

$$\tau_{SC}^{-1} = 2(n_{ph} + n_T)\tilde{\gamma}, \tag{4}$$

where n_T is the equilibrium density of QP, n_{ph} is the density of photoinduced QPs (equivalent to the density of hot phonons), and $\tilde{\gamma}$ is the effective relaxation rate of hot phonons to thermal equilibrium. The essential point of this equation is the relaxation rate determined by the total density of QPs. At the lowest temperature, τ_{SC}^{-1} is governed by n_{ph}, which accounts for the dependence on the photoexcitation fluence demonstrated in the next subsection (Sec. III B). When increasing the temperature, the thermal phonons increase the effective phonon density for QP relaxation, and thus increase τ_{SC}^{-1}. When approaching T_c, τ_{SC}^{-1} is dominated by the phonon relaxation rate $\propto \Delta_{SC}$, resulting in a divergent-like increase of τ_{SC}. Assuming the T-independent $\tilde{\gamma}$, we fit the low-T data very well with Eq. (4) shown by the thin line in Fig. 3(a). Here, we used n_{ph} extracted from the measured T dependence of amplitude [see Fig. 2(a)] and $n_T = N(0)\sqrt{2\pi\,\Delta_{SC}(T)k_BT}\exp[-\Delta_{SC}(T)/k_BT]$ using $\Delta_{SC}(T)$ given by the BCS functional form. From the fit, we obtained $\Delta_{SC}(0) = 4.3$ meV, which is significantly smaller as compared with $\Delta_{SC}(0) = 24$ meV estimated from the fit to the T dependence of the amplitude. Similar underestimation was observed by Kabanov *et al.*,[8] where they suggested that both the assumption of temperature-independent $\tilde{\gamma}$ and the underestimate of the laser heating lead to a reduction of $\Delta_{SC}(0)$. However, we can exclude the latter contribution, especially in the measurement with low pump fluence, because of both the low repetition rate of the laser and identical T_c of $\Delta R/R(T)$ at various fluences demonstrated in the inset of Fig. 2(a). Thus we can attribute the inconsistency between the fit of the temperature dependence of τ and the experimental data to the fact that the model does not account for external processes of phonon escape, particularly those associated with nanoscale textures (stripes).[31]

B. Pump-fluence dependence

SC and PG $\Delta R/R$ transients at 10 K are shown in Figs. 4(a) and 4(b) for various pump fluences $\mathcal{F}$. While the PG component shows qualitatively identical transients at all fluences, the SC component shows changes with increasing $\mathcal{F}$: faster relaxation and saturation of the amplitude together with the appearance of an additional positive component. The saturation behavior has been observed in various superconductors and ascribed to the destruction of the superconducting condensate.[6,11,24,25] In the present case, the additional positive component appearing at higher $\mathcal{F}$ is attributed to the PG that exhibits higher saturation threshold and therefore becomes dominant after the saturation of the SC component.[6]

For the comprehensive assignment of coexisting SC and PG components, we show the T dependence of $\Delta R/R$ transients at $E_{pu}/E_{pr} = 0.95/1.55$ eV with $\mathcal{F}$ above the saturation condition in Fig. 5. The raw data set shown in (a) and (c) indicate that there is a temperature-independent component (instantaneous negative response) that remains above T^*.

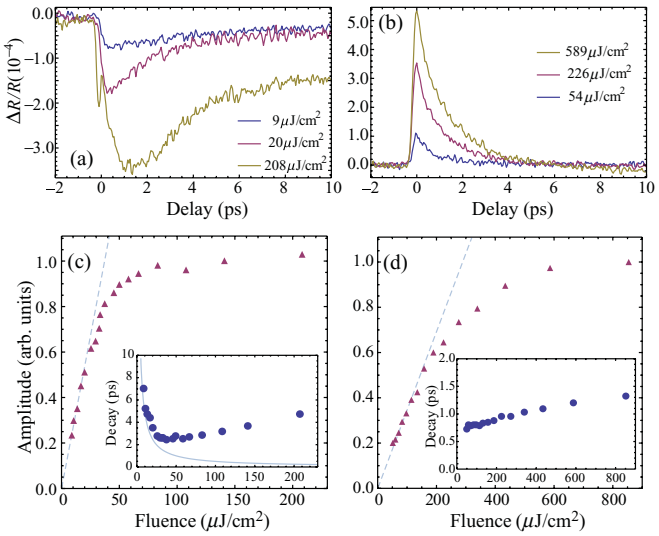

FIG. 4. (Color online) $\Delta R/R$ transients at 10 K excited by various pump fluences with (a) $E_{pu}/E_{pr} = 0.95/1.55$ eV and (b) $E_{pu}/E_{pr} = 1.55/0.95$ eV and $\mathbf{E_{pr}} \parallel a$. (c) and (d) Fluence dependencies of amplitudes and decay times (insets) for the corresponding excitation conditions. The saturation threshold fluence $\mathcal{F}_{th}$ for destructing the superconducting condensate in the excited volume was estimated to be 16 μJ/cm^2 from (c). In the saturation regime, the decay times of SC (τ_{SC}) obtained from the standard exponential fitting are overestimated. The correction of τ_{SC} will be presented in Fig. 6(c).

We removed this component in (b) and (d) by subtracting $\Delta R/R$ transient at $T = 260$ K from the original ones at all temperatures. The additional component is nearly identical to the PG responses observed at the reverse pump/probe energies ($E_{pu}/E_{pr} = 1.55/0.95$ eV), confirming the assignment. With increasing temperature above T_c, this PG component reaches its maximum, then gradually decreases, and finally disappears around T^*. On the other hand, below T_c, this component coexists with the native SC component, as has been demonstrated in the previous papers.[7,13–22,27]

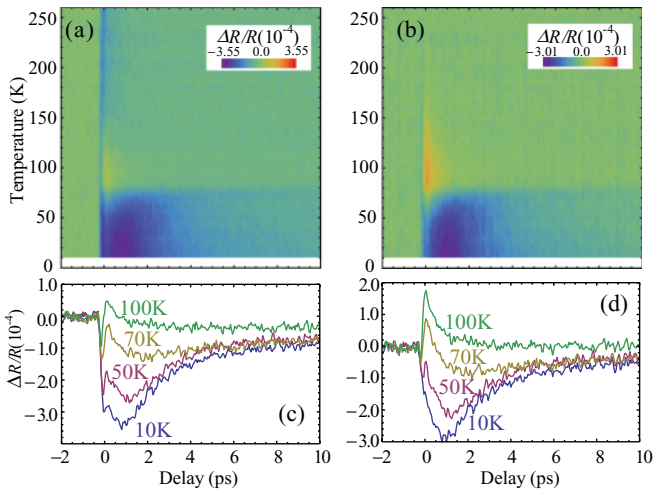

FIG. 5. (Color online) (a) Density plot of $\Delta R/R$ transients as a function of temperature at $E_{pu}/E_{pr} = 0.95/1.55$ eV with $\mathcal{F} = 70$ μJ/cm^2. (b) Density plot after subtraction of T-independent component from (a) by $\Delta R/R(T) - \Delta R/R(T = 260$ K). (c) and (d) Corresponding $\Delta R/R$ transients at typical temperatures.

In Figs. 4(c) and 4(d), we summarize the fluence dependencies of SC ($E_{pu}/E_{pr} = 0.95/1.55$ eV) and PG ($E_{pu}/E_{pr} = 1.55/0.95$ eV) components, respectively. The pump fluence $\mathcal{F}$ varies up to 230 μJ/cm^2 in (c) and 900 μJ/cm^2 in (d). The amplitude of each component shows a saturation with increasing $\mathcal{F}$. According to the inhomogeneous-excitation saturation model established by Kusar *et al.*,[6] we determine the saturation threshold fluence $\mathcal{F}_{th}$ by the value at which $\Delta R/R$ reaches $2\lambda/(1+2\lambda)/(1+\rho^{-2})$ of the maximum of $\Delta R/R$, where $\lambda = \lambda_{pu}/\lambda_{pr}$, with optical penetration depths for pump (λ_{pu}) and probe (λ_{pr}), and $\rho = \rho_{pu}/\rho_{pr}$, with beam radii for pump (ρ_{pu}) and probe (ρ_{pr}). Using $\lambda = 124/174$ nm for 0.95/1.55 eV, extracted from the reflectance of nearly-optimally-doped Bi2212,[32] and the measured values $\rho = 15/20$ μm for 0.95/1.55 eV, we obtained $\mathcal{F}_{th} = 16$ μJ/cm^2 for the SC component and 80 μJ/cm^2 for the PG component. Note that, for the PG component, the saturation value of $\Delta R/R$ was not clearly determined due to the experimental limit of $\mathcal{F}$, and therefore the exact $\mathcal{F}_{th}$ should be larger than 80 μJ/cm^2.

From $\mathcal{F}_{th}$ for the SC component, we calculate the deposited optical SC-state destruction energy density $U_p/k_B = \mathcal{F}_{th}(1-R)/\lambda_{pu}/k_B = 8.8$ K/Cu, which is much larger than the thermodynamic SC condensation energy of $U_c = 0.5$ K/Cu for UD-Bi2212 ($p \approx 0.12$).[33] As previously suggested by Kusar *et al.*,[6] the discrepancy between U_p and U_c indicates an efficient fast dissipation of the photoexcitation energy by phonons.[6] Let us now consider the $\mathcal{F}$ dependencies of the decay times [insets of Figs. 4(c) and 4(d)]. In contrast to the qualitatively similar $\mathcal{F}$ dependence of the SC and PG amplitudes, the decay times in each component reveal unique $\mathcal{F}$ dependencies, which are similar to those observed in the T dependencies. Indeed, as shown by the thin line in the inset of Fig. 4(c), the reduction of τ_{SC} with increasing $\mathcal{F} < \mathcal{F}_{th}$ is well characterized by Eq. (4) using parameters derived from the T dependence [see Fig. 3(a)]. With further increase of $\mathcal{F}$, the decay time deviates from the model curve, and then increases upward. It is important to note that τ_{SC} in the upward region is slightly overestimated since $\Delta R/R$ transient itself deviates from the single exponential decay. This deviation behavior will be discussed in detail in the next section (Sec. III C). On the other hand, τ_{PG} shows a modest increase with increasing $\mathcal{F}$ from 0.7 ps at the lowest $\mathcal{F}$ to ~1.4 ps at the highest $\mathcal{F}$.

C. Dynamics of superconducting condensate at $\mathcal{F} \gg \mathcal{F}_{th}$

In this section, we concentrate our attention to the SC dynamics above the saturation condition at $E_{pu}/E_{pr} = 0.95/1.55$ eV. Figure 6(a) shows $\Delta R/R$ transients excited with various $\mathcal{F} > \mathcal{F}_{th}$ at 10 K, where, due to the saturation of the SC component, the contribution of the PG component becomes apparent as a positive peak together with an instantaneous negative peak that exists throughout the whole temperature range as mentioned in Fig. 5(a). The most striking feature of the saturated dynamics in the SC component is the appearance of a delay preceding the onset of the SC component recovery marked by arrows in Fig. 6(a).

In order to minimize the PG component contribution to $\Delta R/R$ in the delay region at high $\mathcal{F}$ to obtain better insight

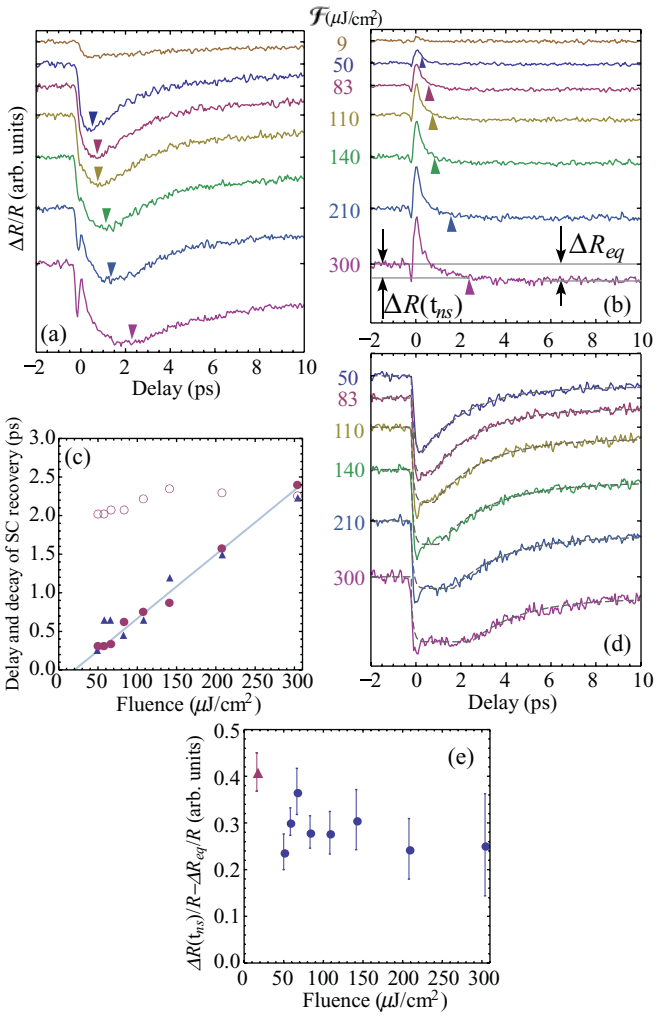

FIG. 6. (Color online) Typical $\Delta R/R$ transients at $E_{pu}/E_{pr} = 0.95/1.55$ eV with various $\mathcal{F} > \mathcal{F}_{th}$ (a) at 10 K ($<T_c$) and (b) at 90 K ($>T_c$). Each plot is shifted vertically. For comparison, $\Delta R/R$ obtained with the lowest $\mathcal{F}$ are shown in the top. (c) Plot of the exponential decay time (τ_{SC}, open circles) and the delay of the exponential decay (t_{ns}, closed circles and triangles) as a function of $\mathcal{F}$. The positions of t_{ns} are indicated by arrows in (a) and (b). (d) $\Delta R/R(T = 10\,\text{K}) - C\Delta R/R(90\,\text{K})$ fitted with a delayed exponential decay (dashed line), where C is $\Delta R_{PG}(10\,\text{K})/\Delta R_{PG}(90\,\text{K}) \approx 1.3$. (e) $\Delta R(t_{ns})/R - \Delta R_{eq}/R$ at 90K, where $\Delta R_{eq}/R$ is defined in (b). The amplitude of the PG component at $\mathcal{F}_{th}$ is also shown (triangle). The error bars represent the standard deviation noise of $\Delta R/R$.

into the prerecovery evolution of the SC component, we subtract the transients measured above T_c [at $T = 90$ K shown in Fig. 6(b)] from the transients measured at 10 K. To compensate for the T dependence of the PG amplitude at low T, $\Delta R/R(90\,\text{K})$ is multiplied before subtraction by $C(T) = \Delta R_{PG}(T)/\Delta R_{PG}$ (90 K) [$C(10\,\text{K}) = 1.3$], derived from the T-dependent amplitude of the PG component in Fig. 2(b). Here, we assumed that the PG amplitude T dependence does not significantly change with $\mathcal{F}$ due to the near-linear $\mathcal{F}$ dependence of the PG component up to $\sim$200 μJ/cm^2. Also note that the above manipulation is correct only under the assumption that the PG decay time is temperature independent.

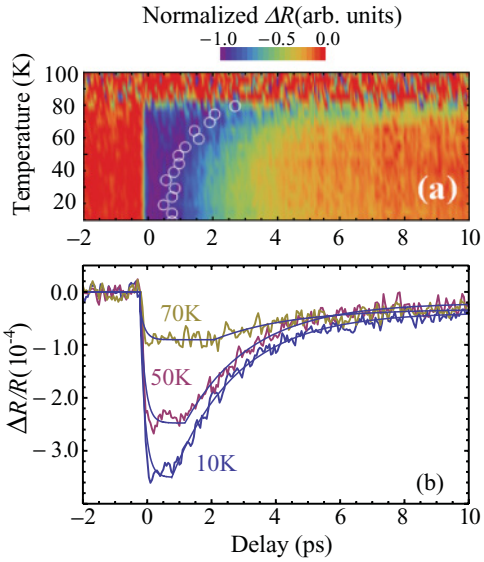

FIG. 7. (Color online) (a) Normalized density plot of $\Delta R/R(T) - C(T)\Delta R/R(T = 90\,\text{K})$ at $E_{pu}/E_{pr} = 0.95/1.55$ eV with $\mathcal{F} = 70\ \mu\text{J/cm}^2$. $C(T) = \Delta R_{PG}(\text{T})/\Delta R_{PG}(90\,\text{K})$ is the calibration coefficient for the T-dependent amplitude of the PG component. (b) Subtracted $\Delta R/R$ transients at typical temperatures. Each transient is fitted by an exponential function delayed by t_{ns}. White circles show t_{ns} obtained from the delayed exponential fits in (b). The raw data (before subtraction) are shown in Fig. 5(a).

The subtracted transients [shown in Fig. 6(d)] show at the highest $\mathcal{F}$ a flat-top response, which follows the initial negative $\sim$100 fs peak. While it is not clear whether the initial peak is an artifact of the subtraction procedure,[34] the flat-top response seems a quite robust feature, since it is consistently present also in T-dependent subtracted intermediate-$\mathcal{F}$ transients shown in Fig. 7.

The $\mathcal{F}$ dependence of the flat-top duration, t_{ns}, obtained from the delayed-exponential-function fits, is shown by the solid circles in Fig. 6(c) and appears consistent with the shifts of the negative peak position obtained from the raw data (triangles), ensuring the validity of the subtraction procedure. A linear fit to the data shows that the delay of the SC recovery intercepts zero at $\mathcal{F} \approx 20\ \mu\text{J/cm}^2$, which is approximately equal to $\mathcal{F}_{th} \approx 16\ \mu\text{J/cm}^2$, suggesting that the delayed recovery starts with the saturation of the SC response.

From the delayed-exponential fits [dashed lines in Fig. 6(d)], we obtain more accurate values of τ_{SC} in the saturation regime [shown as open circles in Fig. 6(c)], that show a much weaker dependence on $\mathcal{F}$ than τ_{SC} obtained by the nondelayed exponential fit [see inset of Fig. 4(c)].

In Fig. 7 we summarize the T dependence of the saturated SC component dynamics obtained by the subtraction procedure performed on the data of Fig. 5. The flat-top response is clearly visible throughout the whole temperature range below T_c. Unlike the divergent-like increase of the superconducting response duration with increasing T near T_c, the flat-top shows a finite t_{ns} ($\sim$3 ps at $\mathcal{F} = 70\ \mu\text{J/cm}^2$) even in the vicinity of T_c. Note that the delay of SC recovery is confirmed also by the shift of the negative peak in the raw data [see Figs. 5(a) and 5(c)].

The flat-top response indicates, due to the saturation properties of the SC component, that in the excited volume the SC gap is temporarily completely closed and the SC condensate remains completely destroyed during t_{ns}. Despite the unreliability of the subtraction during the initial few hundred femtoseconds, the raw data around the threshold indicate [see Fig. 4(a)] that the SC gap closing happens rather fast on a few hundred fs timescale, which is slightly faster than in $La_{1-x}Sr_xCuO_{4+\delta}$.[6] During the flat-top duration, QPs and hot phonons relax but do not contribute to the SC condensation. The subsequent fast (∼2 ps) partial recovery of the SC condensate indicates that the relaxation, during and immediately after the flat-top response, can not be associated with the heat diffusing thermally out of the experimental volume, but it must be associated with relaxation of a transient nonthermal state of the system characterized by an excess of the high-energy excitations.[23] The existence of the transient nonthermal state is supported also by the absence of an increase of the relaxation time near the saturation threshold, which is observed in the case of the thermal transition near T_c [see Fig. 3(a)].

The two most obvious relaxation pathways in such nonthermal system are (i) the diffusion of hot nonthermal QPs and/or high-frequency phonons out of the experimental volume and (ii) their energy relaxation to the thermal (low-frequency) phonon bath. The lower bound for the timescale of (i) can be estimated on the basis of the measured in-plane low-$\mathcal{F}$ hot-QP diffusion constant in $YBa_2Cu_3O_{6.5}$,[35] $\kappa_{ab} \simeq 20$–24 cm^2/s. In the present case, due to the pancakelike geometry of the excitation volume, only the out-of-plane diffusion can contribute. Taking into account the high anisotropy of UD-Bi2212, the timescale of (i), $\tau_c \gg \tau_{ab} = \lambda_{pu}^2/\kappa_{ab} \simeq 6$ ps, clearly indicates the dominance of process (ii).

Our observations therefore suggest that, after the initial fast closure of the SC gap, the system remains in a transient nonthermal normal state for up to $t_{ns} \sim 2$ ps at the highest excitation density. During this time, the hot nonthermal QPs and high-frequency phonons are cooled by the low-frequency phonon bath. After t_{ns}, the population of the hot QPs and high-frequency phonons drops to such level that the SC condensate (and gap) can start to recover. Due to the nonthermal character of the transient normal state a fundamental question appears: what is the exact pathway of the SC state destruction and recovery?

Recently, it was proposed that the photoinduced transition to the normal state (and back) might be of first order.[24,25] Our data indicate that there is no abrupt changes in the photoinduced reflectivity during the recovery, which would be an indication of the first-order transition. However, the excitation density is, due to the finite penetration depth, highly inhomogeneous and any abrupt changes could be easily smeared out. Moreover, the SC rise-time dynamics is obscured by other components preventing us to reliably observe any fast SC component switching during the SC state destruction. On the basis of the present data and in the absence of a second-order transition model valid at high $\mathcal{F}$, which would fit the data, it is therefore not possible to rule out a first-order transition.

Finally, we comment on the contribution of the PG QPs to the photoinduced SC to non-SC phase transition. Assuming that in the PG state $\Delta R/R(t_{ns})$ directly corresponds to the population of the nonequilibrium PG QPs, we use the data above T_c in Fig. 6(b) to estimate the population of the nonequilibrium PG QPs at the moment when the SC condensate starts to recover. In Fig. 6(e), we therefore plot $\Delta R(t_{ns})/R - \Delta R_{eq}/R$ at 90K, where $\Delta R_{eq}/R$ is the $\Delta R/R$ averaged between 9 and 10 ps [see Fig. 6(b)]. For comparison, the amplitude of the PG component at $\mathcal{F}_{th}$ is also shown [triangle in Fig. 6(e)]. The result shows a virtually constant QP density at t_{ns}, suggesting the existence of a critical PG QPs density level correlated with the start of the SC condensation. In other words, the PG QPs also need to cool below a critical level before the SC condensate can recover, suggesting the correlation between the SC and PG QPs.[36]

It is surprising that the gap recovery starts so fast after the complete gap destruction. However, we note that the recovery time of the SC state is also very fast, a few picoseconds, which is much faster than that of MgB_2 (∼100 ps)[12] and even faster than in $La_{2-x}Sr_xCuO_4$[6] (∼10 ps). Also note that the fast recovery time in Bi2212 was widely observed not only for UD samples,[22,25] but also for the optimally-doped (∼2.5 ps from time-resolved ARPES[7,37]) as well as overdoped samples (∼3.3 ps).[24]

IV. CONCLUSIONS

We investigated the relaxation dynamics of photoexcited quasiparticles (QPs) in UD Bi2212 ($T_c = 78$ K). The transient $\Delta R/R$ dynamics associated with SC and PG QPs were selectively isolated from each other by changing the probe beam energy and polarization, enabling us to evaluate the individual dynamics quantitatively. Below the saturation condition, both the temperature and pump-fluence dependencies of SC transients agree well with those predicted from Rothwarf-Taylor model. From the temperature dependencies, we obtained $\Delta_{SC}(0) = 24$ meV using BCS-type temperature-dependent gap and $\Delta_{PG} = 41$ meV, both of which are consistent with the values obtained from other measurements.

The pump fluence dependence of the SC-component-dominated transients shows a contribution of the PG component above the saturation of the SC component ($\mathcal{F}_{th} = 16\ \mu$J/cm^2), where the SC condensate is fully destroyed within the photoexcited volume. We also found a delay of the SC state recovery whose duration time increases linearly with increasing $\mathcal{F} > \mathcal{F}_{th}$. The delay of the SC state recovery is associated with a picosecond-timescale transient normal state. The subsequent fast (picosecond) partial SC state recovery suggests that the phonon and QP population remain highly nonthermal upon photoexcitation, on a time scale of a few picoseconds. During the nonthermal relaxation phase, the energy relaxation proceeds from the high-energy QPs and phonons, which are strongly coupled to phonons that do not break SC pairs. The latter can be the low-frequency phonons or maybe the phonons in the layer isolated from the Cu-O plane.

ACKNOWLEDGMENTS

Y.T. acknowledges support from the JSPS Excellent Young Researchers Overseas Visit Program. Hokkaido group acknowledges Grant-in-Aid for Scientific Research from JSPS. We would like to thank V.V. Kabanov for fruitful discussions.

[1]M. Oda, N. Momono, and M. Ido, Supercond. Sci. Technol. **13**, R139 (2000), and references therein.
[2]K. Tanaka, W. S. Lee, D. H. Lu, A. Fujimori, T. Fujii, Risdiana, I. Terasaki, D. J. Scalapino, T. P. Devereaux, Z. Hussain, and Z.-X. Shen, Science **314**, 1910 (2006).
[3]T. Kondo, T. Takeuchi, A. Kaminski, S. Tsuda, and S. Shin, Phys. Rev. Lett. **98**, 267004 (2007).
[4]T. Kurosawa, T. Yoneyama, Y. Takano, M. Hagiwara, R. Inoue, N. Hagiwara, K. Kurusu, K. Takeyama, N. Momono, M. Oda, and M. Ido, Phys. Rev. B **81**, 094519 (2010).
[5]V. V. Kabanov, J. Demsar, B. Podobnik, and D. Mihailovic, Phys. Rev. B **59**, 1497 (1999).
[6]P. Kusar, V. V. Kabanov, S. Sugai, J. Demsar, T. Mertelj, and D. Mihailovic, Phys. Rev. Lett. **101**, 227001 (2008); P. Kusar, PhD. Thesis, University of Ljubljana, Slovenia, 2007.
[7]R. A. Kaindl, M. A. Carnahan, D. S. Chemla, S. Oh, and J. N. Eckstein, Phys. Rev. B **72**, 060510(R) (2005).
[8]V. V. Kabanov, J. Demsar, and D. Mihailovic, Phys. Rev. Lett. **95**, 147002 (2005).
[9]A. Rothwarf and B. N. Taylor, Phys. Rev. Lett. **19**, 27 (1967).
[10]C. Gadermaier, A. S. Alexandrov, V. V. Kabanov, P. Kusar, T. Mertelj, X. Yao, C. Manzoni, D. Brida, G. Cerullo, and D. Mihailovic, Phys. Rev. Lett. **105**, 257001 (2010).
[11]L. Stojchevska, P. Kusar, T. Mertelj, V. V. Kabanov, Y. Toda, X. Yao, and D. Mihailovic, Phys. Rev. B **84**, 180507 (2011).
[12]J. Demsar, R. D. Averitt, A. J. Taylor, V. V. Kabanov, W. N. Kang, H. J. Kim, E. M. Choi, and S. I. Lee, Phys. Rev. Lett. **91**, 267002 (2003).
[13]T. N. Thomas, C. J. Stevens, A. J. S. Choudary, J. F. Ryan, D. Mihailovic, T. Mertelj, L. Forro, G. Wagner, and J. E. Evetts, Phys. Rev. B **53**, 12436 (1996).
[14]J. Demsar, B. Podobnik, V. V. Kabanov, Th. Wolf, and D. Mihailovic, Phys. Rev. Lett. **82**, 4918 (1999).
[15]Kaindl, M. Woerner, T. Elsaesser, D. Smith, J. Ryan, G. Farnan, M. McCurry, and D. Walmsley, Science **287**, 470 (2000).
[16]H. Murakami, T. Kiwa, N. Kida, M. Tonouchi, T. Uchiyama, I. Iguchi, and Z. Wang, Europhys. Lett. **60**, 288 (2002).
[17]D. Dvorsek, V. V. Kabanov, J. Demsar, S. M. Kazakov, J. Karpinski, and D. Mihailovic, Phys. Rev. B **66**, 020510 (2002).
[18]N. Gedik, P. Blake, R. C. Spitzer, J. Orenstein, R. Liang, D. A. Bonn, and W. N. Hardy, Phys. Rev. B **70**, 014504 (2004).
[19]P. Kusar, J. Demsar, D. Mihailovic, and S. Sugai, Phys. Rev. B **72**, 014544 (2005).
[20]G. Bianchi, C. Chen, M. Nohara, H. Takagi, and J. F. Ryan, Phys. Rev. Lett. **94**, 107004 (2005).
[21]L. Perfetti, P. A. Loukakos, M. Lisowski, U. Bovensiepen, H. Eisaki, and M. Wolf, Phys. Rev. Lett. **99**, 197001 (2007).
[22]Y. H. Liu, Y. Toda, K. Shimatake, N. Momono, M. Oda, and M. Ido, Phys. Rev. Lett. **101**, 137003 (2008).
[23]M. Beyer, D. Städter, M. Beck, H. Schäfer, V. V. Kabanov, G. Logvenov, I. Bozovic, G. Koren, and J. Demsar, Phys. Rev. B **83**, 214515 (2011).
[24]G. Coslovich, C. Giannetti, F. Cilento, S. Dal Conte, G. Ferrini, P. Galinetto, M. Greven, H. Eisaki, M. Raichle, R. Liang, A. Damascelli, and F. Parmigiani, Phys. Rev. B **83**, 064519 (2011).
[25]C. Giannetti, G. Coslovich, F. Cilento, G. Ferrini, H. Eisaki, N. Kaneko, M. Greven, and F. Parmigiani, Phys. Rev. B **79**, 224502 (2009).
[26]C. Giannetti, F. Cilento, S. Dal Conte, G. Coslovich, G. Ferrini, H. Molegraaf, M. Raichle, R. Liang, H. Eisaki, M. Greven, A. Damascelli, D. van der Marel, and F. Parmigiani, Nat. Commun. **2**, 353 (2011).
[27]T. Mertelj, V. V. Kabanov, C. Gadermaier, N. D. Zhigadlo, S. Katrych, J. Karpinski, and D. Mihailovic, Phys. Rev. Lett. **102**, 117002 (2009).
[28]R. Yusupov, T. Mertelj, V. V. Kabanov, S. Brazovskii, P. Kusar, J.-H. Chu, I. R. Fisher, and D. Mihailovic, Nat. Phys. **6**, 681 (2010).
[29]H. Krakauer and W. E. Pickett, Phys. Rev. Lett. **60**, 1665 (1988); M. S. Hybertsen and L. F. Mattheiss, *ibid*. **60**, 1661 (1988).
[30]D. C. Mattis and J. Bardeen, Phys. Rev. **111**, 412 (1958).
[31]D. Mihailovic, Phys. Rev. Lett. **94**, 207001 (2005).
[32]M. A. Quijada, D. B. Tanner, R. J. Kelley, M. Onellion, H. Berger, and G. Margaritondo, Phys. Rev. B **60**, 14917 (1999).
[33]J. W. Loram, J. L. Luo, J. R. Cooper, W. Y. Liang, and J. L. Tallon, Physica C **341**, 831 (2000); T. Matsuzaki, N. Momono, M. Oda, and M. Ido, J. Phys. Soc. Jpn. **73**, 2232 (2004).
[34]The T-independent negative peak, which is observed at high T [see Figs. 5(a) and 5(c)] might be overestimated by the scaling by C.
[35]N. Gedik, J. Orenstein, Ruixing Liang, D. A. Bonn, and W. N. Hardy, Science **300**, 1410 (2003).
[36]On the basis of this scenario, one can expect the T-independent t_{ns}, which is confirmed in the T range below ∼50 K of Fig. 7. The increase of t_{ns} (decrease of PG QPs at t_{ns}) above $T \sim 50$ K could be explained by the increasing number of the thermal PG QPs.
[37]R. Cortes, L. Rettig, Y. Yoshida, H. Eisaki, M. Wolf, and U. Bovensiepen, Phys. Rev. Lett. **107**, 097002 (2011).